IOSR Journal of Electronics and Communication Engineering (IOSR-JECE)
e-ISSN: 2278-2834,p- ISSN: 2278-8735.Volume 17, Issue 5, Ser. I (Sep. – Oct. 2022), PP 27-37
www.iosrjournals.org

Utilizing Phase Congruency Concept-based Algorithm as an Error Mitigation Technique for UWB Signals in Multipath Fading Channels

Nader M. Abdelaziz
Applied College - Jazan University
Jizan, Saudi Arabia
E-mail: alprofinfinity@gmail.com

Abstract**—***this paper evaluates the performance of a newly introduced Error mitigation technique utilizing Phase-Congruency (PC) concept that is usually used in image processing for optimizing the reception performance of Ultra-wideband (UWB) signals in dense Multipath fading channel model using Selective-RAKE Receiver in presence of Multiple-User-Interference (MUI). System models used in this paper are based on both Direct-Sequence and Time-Hopping as spreading techniques for the UWB Pulses. UWB System presented in this paper studied the performance of RAKE Receiver with different number of RAKE Fingers. The analysis and simulation have been run using the 6th derivative of UWB Gaussian pulse which is the new Pulse Shape studied in the paper. The analysis shows that; the UWB pulse-shape and also the number of RAKE fingers have a definite broad effect on the SNR and consequently the BER performance in the multipath fading channel. Finally, the paper concludes that the proposed Phase-Congruency concept-based algorithm is more efficient since it provides better TOA estimation for UWB rays and clusters, and its BER performance is better in the interference-rich environments.*

Index Terms**—** *Bit-Error-Rate (BER), Phase-Congruency (PC), Direct-Sequence (DS), Federal-Communication-Commission (FCC), Multiple-User-Interference (MUI), Signal-to Noise-Ratio (SNR), Time-Hopping (TH), Ultra-Wideband (UWB), Power-Spectral-Density (PSD).*

Date of Submission: 10-09-2022 Date of Acceptance: 28-09-2022

I. INTRODUCTION

ULTRA-WIDEBAND (UWB) technology is a new promising technique for future data communication systems and also for high-accuracy indoor geo-location devices and sensor applications. UWB technology utilizes a carrier-less transmission with very low Power-Spectral-Density (PSD) and an extremely wide spectrum bandwidth; these transmission features resulting from the fact that UWB systems are based on transmission of a very narrow (sub-nanoseconds level) short pulse. The extremely narrow pulses spread the transmitted signal energy over the inherited large frequency spectrum bandwidth. According to the FCC regulation report which states that; "a signal is defined as an UWB signal if it has a -10dB fractional bandwidth (F_{BW}) greater than or equal to 0.20, or the signal occupies at least 500 MHz of frequency spectrum [1]", F_{BW} can be expressed using the following equation

$$F_{BW} = 2 \cdot \frac{f_H - f_L}{f_H + f_L} \geq 0.20 \cdots\cdots\cdots \quad (1)$$

where; f_H and f_L correspond to the high and low frequencies of the -10 dB signal's bandwidth. UWB impulse radio systems utilize its extremely large 7.5 GHz operational bandwidth (from 3.1- to – 10.6 GHz) to convey the signals; that's why UWB is termed as "*Spread Spectrum*" technique despite the fact mentioned above that UWB radio is a carrier-less technique [2]. This paper discusses and compares the UWB systems' performances using different *Pulse Shapes* with two different *Transmission Techniques* which are (DS-UWB) and (TH-UWB) in the IEEE802.15.3a channel model for indoor (short-range) UWB propagation in the presence of both MUI and Gaussian-Noise. The UWB system's evaluation is based on BER vs. SNR signal performance simulation results utilizing RAKE receiver with different number of RAKE fingers also to study the effect of that on system's performance.

Phase-Congruency (PC) concept usually describes the behavior or response of the image *which can be considered as a signal composed of many frequency components* in the frequency domain. It has been noted that edge like features in images have many of their frequency components in the same phase (in-phase) [11][12].

The concept is similar to coherence, except that it applies to functions of different wavelength or frequencies. For example, the Fourier decomposition of a square wave consists of sine functions, whose frequencies are odd multiples of the fundamental frequency. At the rising edges of the square wave, each sinusoidal component has a rising phase; the phases have maximal congruency at the edges [11] as shown in Fig.1. This corresponds to Near-Coherence and total in-phase alignment of frequency components that can be very useful in UWB signal Detection in dense Multipath Environment; the technique which this paper exploits for further UWB signals reception technique Optimization.

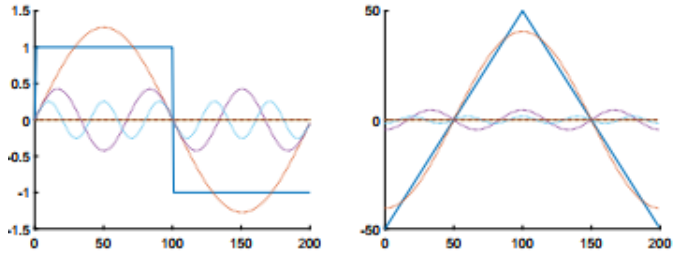

Fig. 1 (a) The first six components of the Fourier series that make up the square signal; (b) the first six components of the Fourier series that make up the triangular signal.

The paper is organized as follows; Sections II provides a brief description of both (DS-UWB) and (TH-UWB) based transmission schemes. UWB Pulse Shape characteristics have been illustrated in Section III. The discussion is followed by describing the UWB propagation channel model under investigation in Section IV. While the Receiver structure and the effect of utilizing Phase-Congruency concept are demonstrated in Section V. Simulation results are explained in Section VI. Finally; Section VII concludes the paper.

II. TRANSMISSION SCHEME & SYSTEM MODEL

A. Direct-Sequence (DS-UWB) Scheme:

A DS-UWB is basically a lot similar to the ordinary DSSS system; the difference is that the Bandwidth spreading effect is achieved by the UWB pulse shaping. The basic format of the DS-UWB for the *k*th impulse radio transmitter (user) output signal is given by:

$$s_{tr}^{(k)}(t) = \sqrt{P_k} \sum_{j=-\infty}^{\infty} \sum_{n=0}^{N_C-1} b_j^{(k)} \cdot c_n^{(k)} \cdot w_{tr}(t - jT_f - nT_c) \quad \ldots. (2)$$

Where; $w_{tr}(t)$ represents the transmitted UWB pulse monocycle, $c_n^{(k)}$ denotes the PN sequence associated to the *k*th user, T_f is the symbol (frame) period, T_c is the chip period such that $T_f = N_c \cdot T_c \cdot b_j^{(k)}$ represents the information bit stream of the *k*th user, P_k is the transmitted power corresponding to the *k*th user , n is an integer= 0,1,2,.., $w_{tr}(t)$ is the UWB transmitted monocycle pulse, $c_n^{(k)}$ represents the PN sequence associated to the kth user, $b_j^{(k)}$ is the data (bit) stream of the *k* th user, T_f is the pulse repetition period (frame time), T_c is the chip period. When utilizing DS techniques in UWB as shown in Fig. (1); a pseudo random code is used to spread the data bit into multiple chips much as conventional DSSS systems, but in UWB systems the pulse waveform takes the role of the "chip" in conventional DSSS systems.

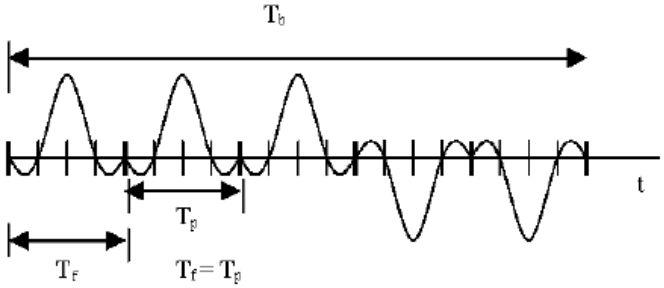

Fig. 2: UWB system based on Direct-Sequence (DS) technique

B. Time-Hopping (TH-UWB) Scheme:

The TH-UWB is identical to the ordinary THSS system which is usually utilizing Pulse-Position-Modulation (PPM) as a modulation scheme. In UWB systems the pulses are assumed to be one of desired UWB pulse shapes mentioned in the previous sub-section. The basic format of the TH using PPM for the *k*th user transmitted signal is given by:

$$s_{tr}^{(k)}(t) = \sum_{j=-\infty}^{\infty} w_{tr}(t - jT_f - c_j^{(k)}T_c - b_j^{(k)}T_{PPM}) \ldots. \quad (3)$$

Where; T_{PPM} represents the pulse time-shift for the Pulse-Position-Modulation (PPM). The time-shift element of the TH code word assigned to the *k*th user is chosen from the set: j= 0,1, 2,.. $N_c - 1$; Where N_c is the number of time-delay bins (chips) in a frame time T_f [8] [2].

All performance measures and simulation results of both DS-UWB and TH-UWB upon reception using RAKE receiver will be discussed and shown later in the simulation results Section.

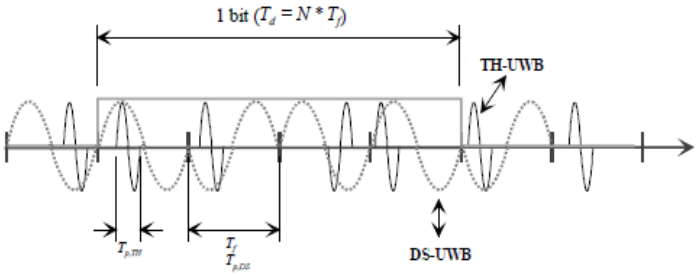

Fig. 3: Basic Concepts of TH-UWB and DS-UWB systems

C. Comparison of DS-UWB & TH-UWB BPM over AWGN Channel:

This sub-Section explains the relative performance of Bi-Phase-Modulation (BPM) for both DS and TH techniques which are shown in Fig. (2) above in an AWGN channel based on the simulation results that will be shown later in the simulation results Section. The BER for up to 15 simultaneous users (interferers) is examined; the synchronous DS system has the pulses for all users transmitted simultaneously, the only feature can be used to suppress MAI is the de-spreading process at the receiver. When asynchronous system is used; the lower cross-correlation values that occur at different pulse alignments means that there is substantially less interference per bit to be suppressed. The performance of both synchronous and asynchronous TH systems are very similar, this is because each user has different pulse transmission instant associated with their PN-sequence; so, the pulses are offset even if the Time-Hopping (TH) frames are aligned (Synchronized).

III. UWB PULSE SHAPE CHARACTERISTICS

Since the spectrum of the UWB pulse train has energy spikes or contains strong spectral peaks at multiples of the pulse repetition frequency, and the regularity of these energy spikes may interfere with other communication systems at short range; then randomizing techniques such as DS and TH are strongly needed to minimize these energy peak lines and consequently mitigate the interference with other communication systems (MAI). Moreover, the randomizing techniques mentioned are also used as a multiple access method. But one of the most important features that play an important role in the UWB communication system quality and controls UWB signals' performance through transmission and propagation over the expected wireless multipath channel is the chosen UWB Pulse Shape [3]. The study of the basic pulse shape is fundamental because important performance factors of an UWB system depend on it such as; efficient use of permitted emission power (PSD), coexistence with other radio communication systems and a simple circuit implementation.

One of the fundamental challenges is to maximize the radiated energy of the transmitted UWB pulse while its power spectral density still complies or "fit in" with the spectral power regulations of the FCC mask which regulated the use of the UWB devices respecting the emission limit values as shown in Fig. (3) [2]. Due to the extremely low emitted power level currently allowed in the FCC part 15 report; the UWB systems are considered suitable for short-range and indoor applications because they operate best over short distances of about 2 – 3 meters delivering data speeds of 480 Mbps, and as distance increases; the speed decreases, but at 10 meters speed still reaches or exceeds 100 Mbps.

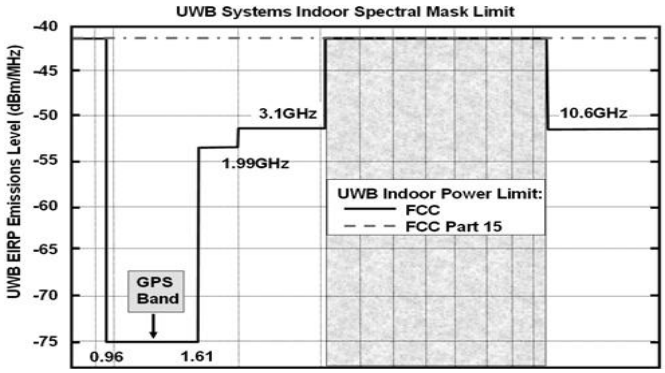

Fig. 4: UWB indoor emission mask regulated by FCC

The basic pulses used in simulation of this study paper are derivatives of the *Gaussian pulse* which can be expressed as shown in Equation (4):

$$y_{Gn}(t) = \frac{d^n}{dt^n}\left(A \cdot \exp(\frac{t}{\eta})^2 \right) \qquad \text{……..} \qquad (4)$$

Where; A is the normalized Pulse amplitude, and η is the time-scaling factor and its relation to the pulse width T_P is that $T_P = 7\eta$ which contains about 99.98% of the total pulse energy. To ensure that the frequency spectrum of the pulse fulfills the FCC PSD requirement; the appropriate derivative and the decaying factor have to be chosen carefully. As shown in Fig. (4) the different order pulse derivatives based on the *Gaussian pulse* have been used to select an optimum pulse decaying factor of 0.167 ns. This has been calculated following the bi-section method approach as shown in [4].

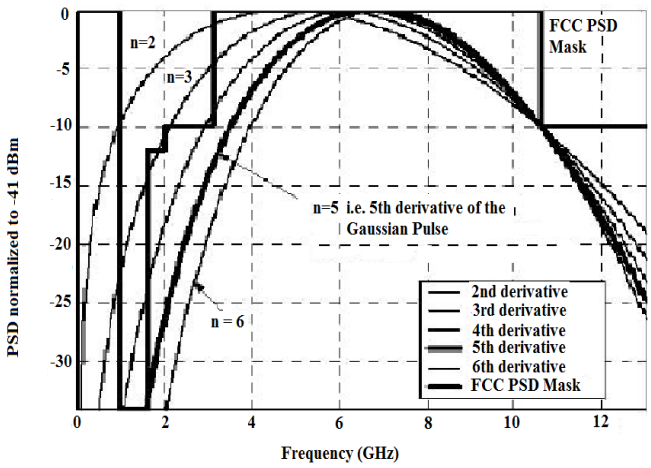

Fig. 5: PSDs of higher order derivatives of UWB Gaussian pulses

More waveforms can be created as mentioned before by a sort of high-pass filtering of the main *Gaussian pulse* which acts in a manner similar to taking the derivative of it. When the *Gaussian pulse* is transmitted; due to the derivative characteristics of the transmitter antenna the output can be modeled by the first derivative of the *Gaussian pulse* [3]. Therefore, the pulse radiated will be the 1st derivative of the *Gaussian pulse* which is known as *monocycle*. But the PSD of the *Gaussian monocycle* does not meet the FCC mask requirements. Therefore, new pulse shapes must be found to satisfy the FCC requirements. So, one approach to achieve that is to generate higher order derivatives of the *Gaussian pulse*, this approach leads to considering higher-order derivatives of the *Gaussian pulse* as candidates for UWB transmission, especially by choosing the order of the derivative and a suitable pulse width; we can find a pulse that satisfies the FCC's mask requirements while maximizing the pulse's energy to deliver more data for longer distances. A *Gaussian-doublet* is the second derivative of the *Gaussian pulse* and it is the most popular and most used in the UWB literature researches which is given by the equation:

$$y_{G2}(t) = \left(1 - 4\pi(\frac{t}{\eta})^2\right) \cdot \exp\left(-2\pi(\frac{t}{\eta})^2\right) \quad \ldots\ldots \quad (5)$$

Where; $-\infty < t < \infty$, η is the time-scaling factor. We have to mention that further derivatives of the *Gaussian pulse* yield additional zero-crossings as one additional zero-crossing for each additional "further" derivative. Also, if the value of the time-scaling factor η is fixed; then by taking an additional derivative the fractional bandwidth F_{BW} decreases as a result to the center frequency f_C increase, which is shown in equation (6) below:

$$f_C = \frac{f_H + f_L}{2} \quad \ldots\ldots\ldots\ldots\ldots\ldots \quad (6)$$

In time-domain the observations prove that the duration of the pulse remains the same for various high-order derivatives considering $T_P = 7\eta$ for all pulses. The chosen pulse shape for analyzing the performance evaluation in this paper is the 6th derivative of the *Gaussian pulse* which is given by the following equation:

$$y_{G6}(t) = \left(1 - 12\pi \cdot (\frac{t}{\eta})^2 + 16\pi^2 \cdot (\frac{t}{\eta})^4 - \frac{64}{15}\pi^3 \cdot (\frac{t}{\eta})^6\right) \cdot \exp\left(-2\pi \cdot (\frac{t}{\eta})^2\right) \ldots\ldots \quad (7)$$

However, results show that the pulse width will be less than 1 nanosecond, the peak center frequency reaches 7.2 GHz which increases with the square root of order of the derivative, and the maximum PSD can be controlled by changing the normalized amplitude A of the pulse. Taking to consideration that the derivative operation could be implemented as high pass filtering process of the previously lower order of the *Gaussian pulse*; to transmit the 6th derivative over air-interface, the *Gaussian pulse* must be filtered to the 5th order derivative [3].

IV. UWB PROPAGATION CHANNEL MODEL

The modified Saleh-Valenzuela (S-V) model was adopted as a reference UWB channel model by the IEEE 802.15.3 in 2003 [5]. The modeling of UWB propagation channels is based on the measurements of indoor propagation environment as the main commercial application. The distinguishing features of UWB propagation channel are its extremely multipath-rich profile and non-Rayleigh fading characteristics. As for the propagation channel of UWB signals considered in this paper; it is the UWB multipath Non-Line-Of-Sight (NLOS) indoor channel based on the modified Saleh-Valenzuela (S-V) model, which taking into account the "Clustering" phenomenon observed at the UWB indoor data measurements in each of the different paths from transmitter to the receiver. As the bandwidth of the UWB waveforms can be ultra wide; different parts of the same object in the indoor environment can give rise to several multipath components all of which would be parts of one single "Cluster". Thus, the multipath components arrive at the receiver in clusters, and within each cluster there are multiple subsequent arrivals called "rays" [5][6]. Therefore, for the time-of-arrival (TOA) statistics the IEEE 802.15.3a standard channel model used modified Saleh-Valenzuela (S-V) model approach that characterizes multipath components in clusters and rays.

So, the multipath channel impulse response can be represented as:

$$h_i(t) = X_i \sum_{l=0}^{L_C - 1} \sum_{k=0}^{K_{LC} - 1} \alpha_{k,l} \cdot \delta(t - T_l^i - \tau_{k,l}^i) \ldots\ldots \quad (8)$$

Where; $\alpha_{k.l}^i$ represents the multipath gain coefficients, T_l^i represents the delays of the l th cluster, $\tau_{k,l}^i$ represents the delays of the k th multipath component "ray" within the l th cluster arrival time (T_l^i). Shadowing effect of the total multipath energy is log-normal distributed and is represented by the term X_i, and i refers to the i th realization.

The multipath components are defined in "clusters" and "rays" as described previously. Cluster arrivals are Poisson distributed with "Cluster arrival rate" (Λ). And within each cluster; the ray arrivals are also Poisson distributed with "Ray arrival rate" (λ), and $\lambda >> \Lambda$. The model illustration assumes that within a cluster; the first ray arrives with no delay ($\tau_{0,l} = 0$). The distributions of cluster arrival time and ray arrival time are expressed in the equations (9) and (10) [5]:

$$p(T_l \setminus T_{l-1}) = \Lambda \cdot \exp(-\Lambda \cdot (T_l - T_{l-1})) \ldots\ldots \quad (9)$$

$$p(\tau_{k,l} \setminus \tau_{(k-1),l}) = \lambda \cdot \exp(-\lambda \cdot (\tau_{k,l} - \tau_{(k-1),l})) \ldots \quad (10)$$

Where $k > 0$.

The IEEE 802.15.3a standard multipath channel proposal defined four different models for four different scenarios of measurement environments; namely CM1, CM2, CM3, CM4; which characterized as follows:

- CM1: Line-Of-Sight (LOS) model for distance 0 – 4 m.
- CM2: Non-LOS (NLOS) model for distance 0 – 4 m.
- CM3: NLOS for distance 4 – 10 m.
- CM4: NLOS for distance 4 – 10 m, with extreme (dense) multipath channel condition.

V. RAKE RECEIVER STRUCTURE AND PHASE-CONGRUENCY CONCEPT UTILIZATION

One of the most attractive features of UWB communications is the ability to resolve multipath, numerous investigations have confirmed that the impulse radio UWB channel can be resolved into significant number of multipath components. A Rake receiver can be employed to exploit the multipath diversity using many reception algorithms; for instance, the Rake receiver using Maximum-Ratio-Combining (MRC) is considered optimum only when the disturbance to desired UWB signal is coming from Additive-White-Gaussian-Noise (AWGN) [8], [10].

The most important application of UWB communications is as a physical layer of the emerging wireless personal area networks (WPANs) which will be required to operate in proximity to other networks such as LANs. Hence; the presence of narrowband interference emitted by other networks made the conventional Rake receiver combiner shown in Fig. 6 below an unsuitable for reception because it will exhibit an error floor dependent on the signal-to-interference ratio (SIR) [9]. A more suitable scheme to employ in this case is "Optimum-Combining" (OC) Rake receiver; in which the received UWB multipath component signals are weighted on each component "path" basis in each Rake finger, and then these components are combined to maximize the output signal-to-interference plus noise ratio (SINR). Commonly Rake receivers are employed in UWB systems to collect energy from different multipath components, a Rake receiver combining all the paths of the incoming signal is called "All-Rake" (A Rake) receiver presented in Fig. 6 [7]. But since UWB signals have very wide bandwidth then; the (A Rake) receiver is not an efficient practical implementation in this case due its complexity, instead; a feasible implementation of multipath combining has been proposed which called "Selective-Rake" (S Rake) receiver which is shown in Fig. 7 below. The (S Rake) receiver combines the "M" best multipath components of the total "L" multipath components which can be determined by Rake finger selection algorithm [6].

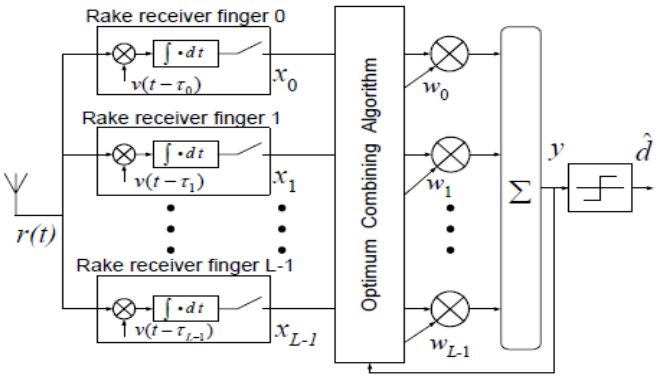

Fig. 6: All-Rake receiver combiner structure

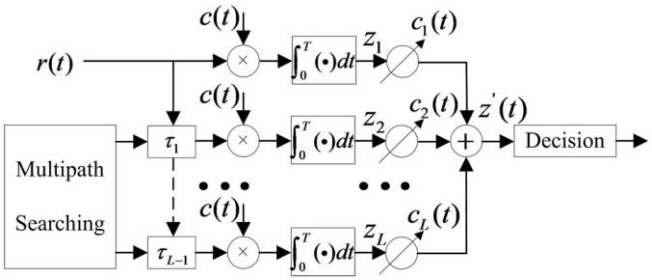

Fig. 7: Selective-Rake receiver structure

In Maximal-Ratio-Combining (MRC) Rake receiver the paths with highest signal-to-noise ratio (SNR) are selected, and by increasing the number of Rake fingers which consequently means increasing the number of resolvable multipath components is a considerable factor that leads to the reception performance optimization.

The main contribution of this paper is to improve the ability of the S Rake receiver utilizing the PC concept to furtherly support the Decision process takes place in the Decision device at the end of the S Rake block diagram. Using the PC concept; at the corners, the tops and bottoms of obstacles in the Extreme (dense) Multipath indoor environment as in the proposed channel model (CM4) in this paper; all the Fourier frequency components of a single ray or cluster of an UWB signal will be in-phase [13].

$$PC_2(x) = \frac{\sum_n W(x)\lfloor A_n \Delta\phi(x) - T \rfloor}{\sum_n A_n(x) + \varepsilon},$$

where

$$\Delta\phi_n(x) = \cos(\gamma_n(x)) - |\sin(\gamma_n(x))|, \quad \ldots (11)$$

Where: $W(x)$ takes care of the frequency spread effect, ε is a small positive constant to avoid division by zero, and T is used to reduce the Noise effect. while the operator $\lfloor \rfloor$ removes negative quantities.

But expectedly; the Fourier frequency components of multiple UWB signal rays or clusters will be extremely dispersed and become out-of-phase regarding each other. Hence, if the PC concept carefully been utilized as an additional algorithm to the S Rake receiver structure; it provides an important and clear measure of distinction between the extremely dispersed rays and clusters of the UWB signal due to reflection and refraction of rays. Moreover, this measure of distinction will provide better Time-Of-Arrival (TOA) estimation for different rays and clusters of UWB signal and thus can be very useful to the "Multipath Searching" mechanism and to adjust the delay-circuits designed by the better estimated TOA for each received path (ray) or cluster of the received UWB Signal at the front-end of the S Rake structure as shown in Fig. 8.

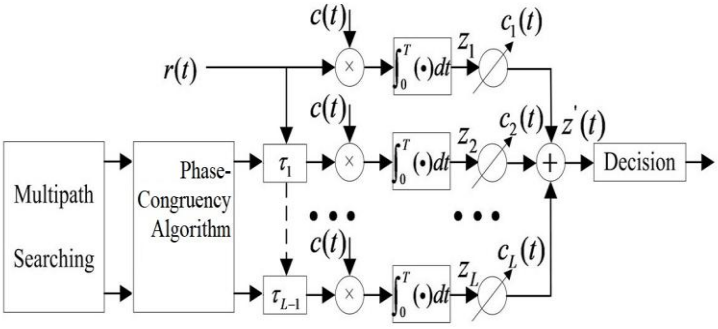

Fig. 8: Selective-Rake receiver structure combined with PC algorithm for the delay-circuits further Adjustment

VI. SIMULATION AND RESULTS

The performance evaluation of the UWB system in this paper is accomplished on the (BER vs. SNR) basis employing the 6th derivative of the *Gaussian pulse* expressed previously in (7), and using S Rake receiver with different number of fingers (arms) utilizing PC concept-based algorithm for better TOA estimation to see the effect on the reception performance. The simulation is performed by MATLAB 13b codes along with SIMULINK library also to compare between the DS and TH-PPM performances in the presence of AWGN along with narrowband interference, all of these interferences are been studied over multipath NLOS channel model based on Saleh-Valenzuela channel model CM4 with dense multipaths.

The narrowband interference is assumed to be coming from IEEE 802.11a WLAN source taking into consideration to be more practical study case because it operates in the 5 GHz range, which is in the bandwidth range of the UWB channel assumed here in the paper.

The paper presents intensive simulation results for the performance of the 6th derivative of the *Gaussian pulse* using DS-UWB and TH-PPM transmission techniques, and employing S Rake receiver with different Rake finger numbers (4 fingers, 8 fingers, and 128 fingers which is considered an infinite number "∞" of fingers) utilizing PC concept-based algorithm, and also the paper examines one of the most efficient algorithms used in adaptive filtering from the MATLAB libraries which is "Recursive Least Squares" (RLS) algorithm. RLS algorithm is an algorithm which recursively finds the filter coefficients that minimize a weighted linear least squares cost function relating to the input signals. In the derivation of the RLS; the input signals are considered

deterministic, and compared to most of its competitors; the RLS exhibits extremely fast convergence. However, this benefit comes at the cost of high computational complexity. The simulation assumes the transmission channel to be UWB indoor (S-V CM4) channel model with BER of order 10^{-4} is the goal of this paper.

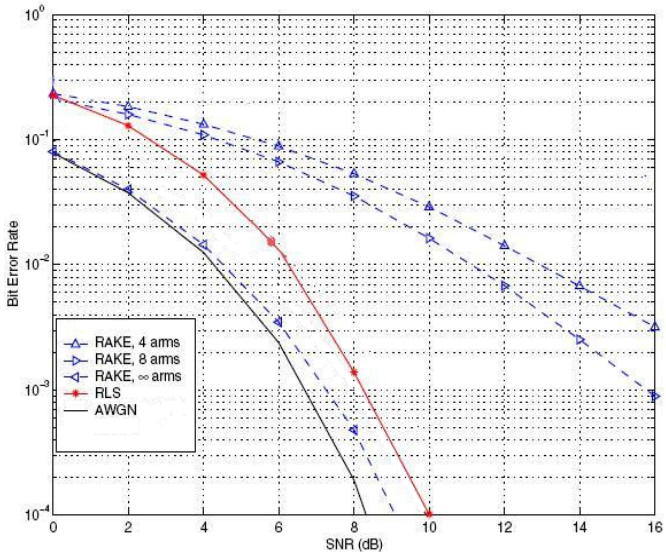

Fig. 9: BER performance of DS-UWB over multipath S-V CM4 channel without interferers

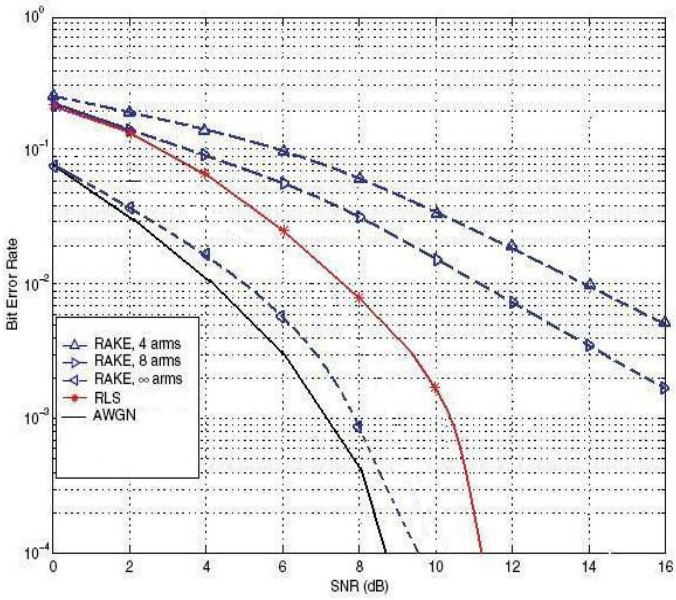

Fig. 10: BER performance of TH-UWB over multipath S-V CM4 channel without interferers

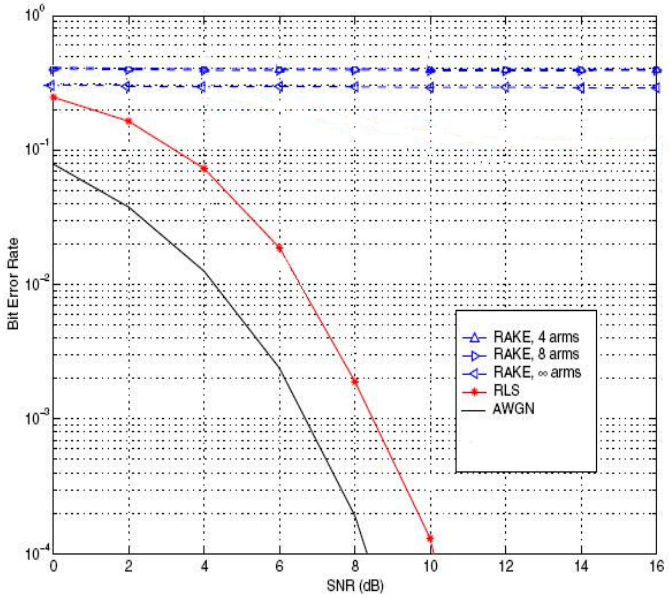

Fig. 11: BER performance of DS-UWB over multipath S-V CM4 channel with single NB interferer (SIR = -30 dB)

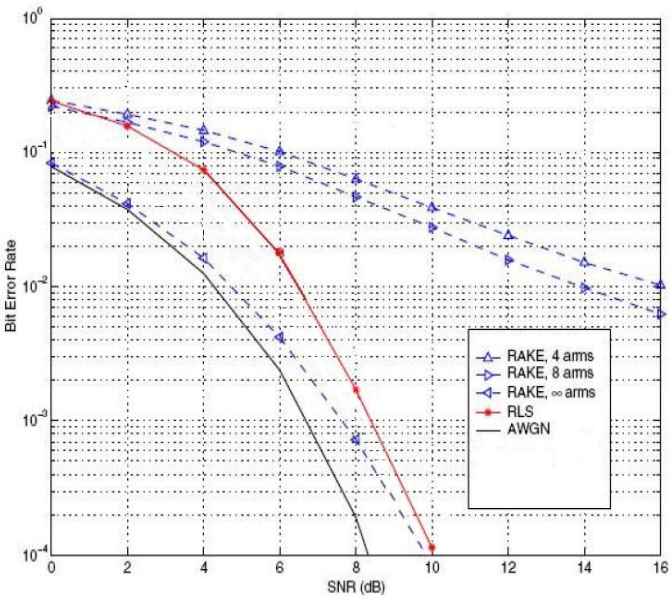

Fig. 12: BER performance of DS-UWB over multipath S-V CM4 channel with single NB interferer (SIR = 0 dB)

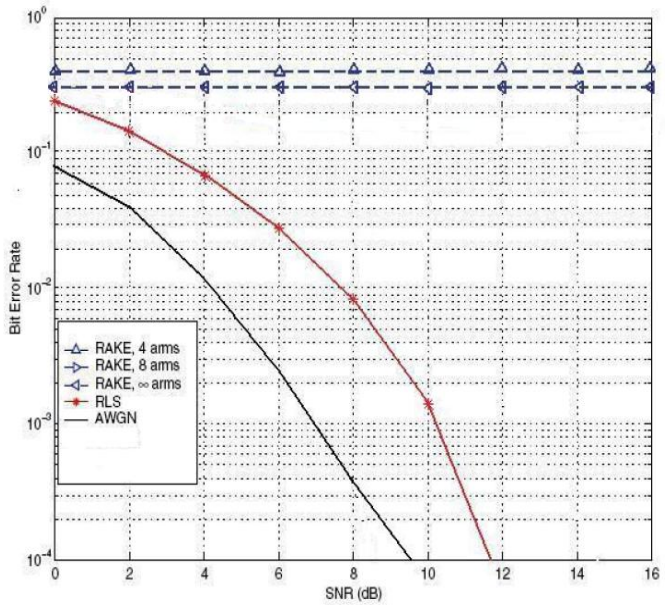

Fig. 13: BER performance of TH-UWB over multipath S-V CM4 channel with single NB interferer (SIR = -30 dB)

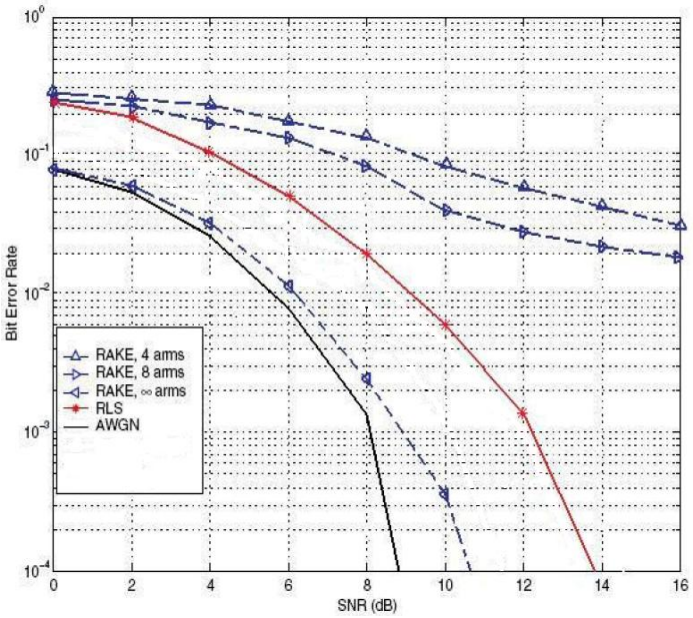

Fig. 14: BER performance of TH-UWB over multipath S-V CM4 channel with single NB interferer (SIR = 0 dB)

The paper has examined the simulation parameters and results in the previous figures; Fig. (7, 8, 9, 10, 11 and 12) for the following three scenarios:

- Multipath NLOS Channel with only AWGN (no Narrowband interference).
- Multipath NLOS Channel with the effect of a single Narrowband interference source with SIR = -30 dB.
- Multipath NLOS Channel with the effect of a single Narrowband interference source with SIR = 0 dB.

VII. CONCLUSION

This paper presents the performance of the 6th derivative of the UWB Gaussian pulse using two different transmission schemes which are DS-UWB by using BPM modulation technique, and TH-UWB using PPM modulation technique. The performance evaluation of the previously mentioned pulse shape using the two different transmission schemes is assumed to experience a multipath fading channel derived by the IEEE 802.15.3a working group from the Saleh-Valenzuela channel model (CM4) which is characterized for NLOS

indoor environment with distance between transmitter and receiver from 4 – 10 meters with extreme Multipath components. Also, the paper studies the effect of both AWGN without any interference, and in the presence of narrowband interference with two study cases of signal-to-interference ratio (SIR = -30 dB, and SIR = 0 dB) on the UWB signal performance. As for reception technique; the paper presents the performance of conventional UWB Rake receiver using Recursive Least Squares (RLS) adaptive algorithm analytically, and more importantly the effect of utilizing Phase-Congruency (PC) concept-based Algorithm in Selective-Rake receiver (S Rake) structure with different number of Rake fingers (4, 8, and 128 or "infinite fingers on the UWB signal's performance based on BER vs. SNR. The simulation results show that; generally, the performance of DS-UWB is better than TH-UWB and especially in the presence of any narrowband interference in addition to AWGN. Moreover, the simulation results prove that increasing the number of S Rake receiver fingers utilizing PC concept-based algorithm leads to more resolvable multipath components which consequently improve the reception performance. However, as the interference power increases (poorer SIR); the performance difference between the two transmission schemes and the performance of different number of Rake fingers become clearer to the observing eye, and that is the reason of examining the three simulation scenarios in details.

REFERENCES

[1]. Ian Oppermann, Matti Hamalainen "UWB Theory and Applications," Book, pp. 15–80.
[2]. M.Ghavami, L.B.Michael "Ultra-Wideband Signals and Systems in Communication Engineering," Book, pp. 26–113.
[3]. Amer Nezirovic, "Parameter Optimization in UWB Impulse Radio for Single User Scenario". New York, Master Thesis 2009, ch.2,3, 4.
[4]. B. M.Mezzour, "Direct Sequence UWB performance over STDL " paper Journal, vol.3.
[5]. Andreas F. Molisch, "UWB Wireless Channels – Propagation Aspects and Interplay with System Design" IEEE Trans. Vol.4 2010.
[6]. Zubair Main Zain, Safdar Hashim, "Performance Evaluation of Rake Receiver Using UWB Multipath Channel," Master Thesis, june 2008.
[7]. G.S.Biradar, S.N.Merchant, Indian Institute of Technology Bombay, "An Adaptive Rake Receiver Algorithms for DS-CDMA IEEE Trans. Vol.3 February 2011.
[8]. Hongsan Sheng, Alexander M. Haimovich, "Optimum Combining for Time-Hopping Impulse Radio UWB Rake Receiver" IEEE Transl. J. vol., Aug. 2009.
[9]. Jiang Lei, Zhang Jianhua, "A Study of UWB Interference at 3G Systems" Master Thesis 2006, Beijing: Beijing University.
[10]. Bikramaditya Das, "Rake-MMSE time domain equalizer for high data rate UWB communication systems"" IEEE Trans. Electron Devices, vol. ED-11, December 2009.
[11]. Muthana Hamd, Rabab Rasool, "Towards better performance: phase congruency-based face recognition", TELKOMNIKA Indonesian Journal of Electrical Engineering 18(6):3041-3049, December 2020.
[12]. Yan Yang, Kit Ian Kou, Cuiming Zou, "Edge Detection Methods Based on Modified Differential Phase Congruency of Monogenic Signal", IEEE Trans. Vol.4 December 2016.
[13]. Xiaojuan Deng, Zuo Feifei, Hongwei Li, "Cracks Detection Using Iterative Phase Congruency", Journal of Mathematical Imaging and Vision 60(2), DOI:10.1007/s10851-018-0796-y, September 2018.

Nader M. Abdelaziz. "Utilizing Phase Congruency Concept-based Algorithm as an Error Mitigation Technique for UWB Signals in Multipath Fading Channels." *IOSR Journal of Electronics and Communication Engineering (IOSR-JECE)* 17(5), (2022): pp 27-37.